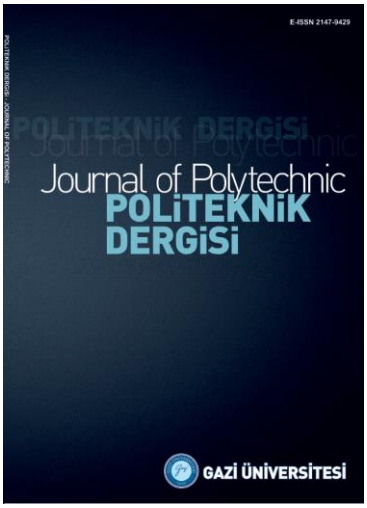

POLİTEKNİK DERGİSİ

JOURNAL of POLYTECHNIC

ISSN: 1302-0900 (PRINT), ISSN: 2147-9429 (ONLINE)
URL: http://dergipark.org.tr/politeknik

Inverse dynamics of bipedal gait: the assumption of the center of pressure as an ınstantaneous center of rotation

İki bacaklı yürüyüşün ters dinamiği : basınç merkezinin bir ani dönme merkezi olduğu varsayımı

***Yazar(lar) (Author(s))**: Fatih CELLEK[1], Barış KALAYCIOĞLU[2]*

ORCID[1]: 0000-0002-9652-9931

ORCID[2]: 0000-0002-1295-3816

Bu makaleye şu şekilde atıfta bulunabilirsiniz(To cite to this article): Cellek F., Kalaycıoğlu B., "Inverse dynamics of bipedal gait: the assumption of the center of pressure as an ınstantaneous center of rotation", ***Politeknik Dergisi***, 25(3): 1023-1032, (2022).

Erişim linki (To link to this article): http://dergipark.org.tr/politeknik/archive

DOI: **10.2339/politeknik.901642**

Inverse Dynamics of Bipedal Gait: The Assumption of the Center of Pressure as an Instantaneous Center of Rotation

Highlights

- *An alternative 2-D, 7-link,7-dof dynamical model for bipedal gait is presented*
- *The support foot is considered as two parts that are active and passive parts*
- *The center of pressure of the support foot is assumed as a hypothetical revolute joint between the foot and the ground*
- *Clinical Gait Analysis Data of Winter are used to verify the analytical approach*

Graphical Abstract

Unlike the rotation about a fixed point, it is assumed that the right foot rotates about the center of pressure (COP) in the Single Support Phase (SSP).

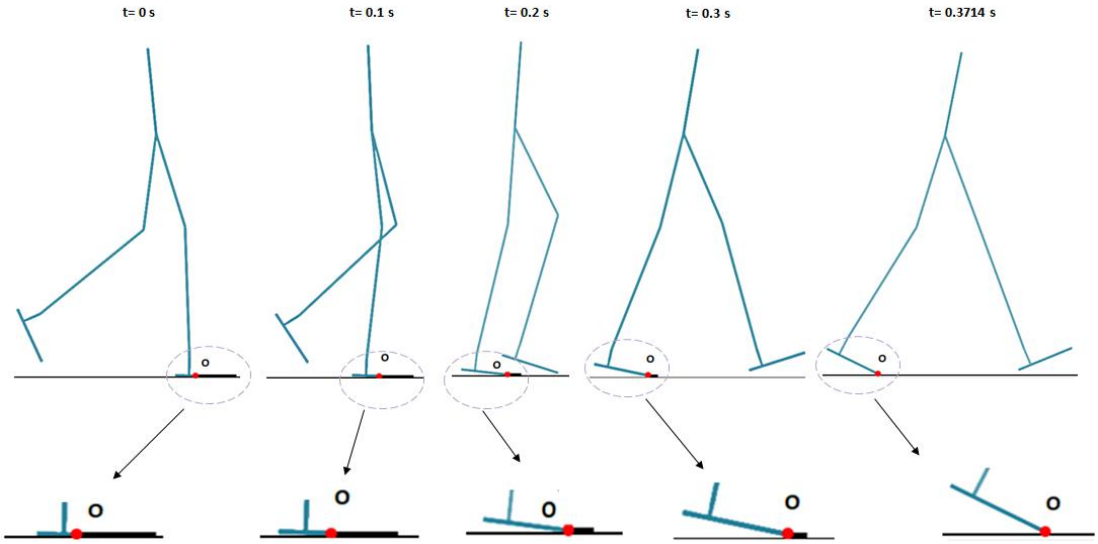

Figure Varying location of the Center of Pressure (COP)

Aim

A more realistic 2-d model of the real human gait is proposed in this study.

Design & Methodology

The equations of motions of the bipedal gait are derived by applying Lagrange equations. Analytical results and clinical gait analysis data of Winter are compared.

Originality

The resultants of ground reaction forces occur on the foot in the COP. It is supposed that this point is a hypothetical revolute joint between the foot and the ground and the foot rotates about this point in the SSP.

Findings

The results calculated for the right and left ankle joints are much closer to the actual values. The errors increase from the lower joints to the upper. The results calculated for the left joints are much closer to the actual values.

Conclusion

Although some errors are observed, the analytical results are close to the clinical gait analysis data. The new approach works well, but further research is needed

Declaration of Ethical Standards

The author(s) of this article declare that the materials and methods used in this study do not require ethical committee permission and/or legal-special permission.

Inverse Dynamics of Bipedal Gait: The Assumption of the Center of Pressure as an Instantaneous Center of Rotation

Araştırma Makalesi / Research Article

Fatih CELLEK*, Barış KALAYCIOĞLU

Faculty of Engineering, Department of Mechanical Engineering, Kırıkkale University, Turkey

(Geliş/Received : 23.03.2021 ; Kabul/Accepted : 13.04.2021 ; Erken Görünüm/Early View : 05.05.2021)

ABSTRACT

In the study, an alternative 7-dof dynamical model that can be used in gait analysis of human, bipedal robots and exoskeleton systems is proposed. The dimensions and kinematic data of the model are specified on the basis of anthropometry and kinematic data of real human gait. The 7-link model consists of the trunk, two thighs, two shanks and two feet links. The movement is examined in the sagittal plane and during the single support phase (SSP). Unlike the rotation about a fixed point, it is assumed that the right foot rotates about the center of pressure (COP). The part between the COP and the tip of the toe is considered to be a passive limb which is horizontally on the ground. The effect of this part on dynamic analysis is neglected. The equations of motions are derived by applying Lagrange equations. Using the kinematic data obtained in clinical gait analysis (CGA) conducted by Winter [1], the net joint torques are calculated and then compared with CGA torque data. As a result of the comparisons, it is seen that the curves are overlapped significantly.

Keywords: Bipedal gait, single support phase, joint torques, center of pressure (COP), instantaneous center of rotation(IC).

İki Bacaklı Yürüyüşün Ters Dinamiği : Basınç Merkezinin Bir Ani Dönme Merkezi Olduğu Varsayımı

ÖZ

Bu çalışmada, gerçek insan, iki ayaklı yürüyen robotlar ve dış iskelet sistemlerinin yürüyüş analizlerinde kullanılabilecek, 2 boyutlu alternatif bir dinamik model önerilmiştir. Modelin boyutları ve kinematik verileri, antropometrik veriler ve gerçek insan yürüyüşünün kinematik verileri esas alınarak belirlenmiştir. 7 uzuvlu model; gövde, iki adet üst bacak (uyluk), iki adet alt bacak (baldır) ve iki adet ayak uzuvlarından oluşmaktadır. Hareket, sagital düzlemde ve tek ayak destek fazında incelenmiştir. Sağ ayağın, sabit bir nokta etrafında dönmesinden farklı olarak, ayak basınç merkezi (COP) etrafında dairesel hareket yaptığı kabul edilmiştir. Basınç merkezi (COP) ile ayak başparmağı ucu arasındaki kısım, yatay olarak yerde hareketsiz bulunan pasif bir uzuv gibi değerlendirilmiştir. Bu kısmın dinamik analize etkisi ihmal edilmiştir. Lagrange denklemleri ile hareket denklemleri elde edilmiştir. Winter [1] tarafından yapılmış klinik yürüyüş deneylerinde elde edilen kinematik veriler kullanılarak, her bir uzvun hareketi için gerekli net mafsal torkları belirlenmiş ve grafikler üzerinde deneysel sonuçlarla karşılaştırılmıştır. Karşılaştırmalar neticesinde, analitik ve deneysel sonuçlardan elde edilen eğrilerin önemli oranda örtüştüğü görülmüştür.

Anahtar Kelimeler: İki ayaklı yürüme, tek ayak destek fazı, mafsal torkları, basınç merkezi, ani dönme merkezi.

1. INTRODUCTION

Bipedal walking or human-like walking is a very important issue that has a major role in the extraordinary advances in robotics technology. Bipedal systems are concentrated on because; they can be better adapted to the living environment compared to other mobile systems with wheels and tracks [2].

Bipedal walking robots and exoskeletons are used for different purposes in defense and manufacturing sectors, especially in health. In the field of health; exoskeletons and robotic systems are used in the rehabilitation of individuals who have partially or completely lost their walking ability and to provide walking support. Also in recent years; It has also started to be used to support soldiers, firemen, heavy industrial workers, search and rescue workers and jobs that need more power than manpower [3,4]. Also, it is benefited from bipedal robots in some areas that push the human limits and that are dangerous such as heavy industry, nuclear and space research [5]. In the future, it is expected to completely replace the human in many industries [6].

These technologies are based on inspirations from human. Although the complicated musculoskeletal system of the human body cannot be imitated exactly,

* *Corresponding Author (Sorumlu Yazar)*
e-posta : fatihcellek@kku.edu.tr

humanoid walking can be performed with fewer degrees of freedom and simplified systems [7,8]. Human gait is a complex of movements that occur with the integration of motor control and the musculoskeletal system. The body moves in sagittal, coronal and transverse planes. Since the angle changes in the coronal and transverse planes are very small compared to the angle changes in the sagittal plane, the motions in the these planes have been neglected in most rehabilitation robots and exoskeleton systems. For this reason, the ankle, knee and hip joints can be modeled as a single degree of freedom revolute joint [9].

Firstly, kinematic data of lower limbs and joints must be obtained to imitate the humanoid gait. Although some analytical approaches, software or simulation results can be used, the most realistic way is to get real human gait data experimentally [10,11]. For this purpose, real linear and angular kinematic data of limbs and joints are determined in clinical gait experiments. In most of the experimental studies in the literature [1,12–16], these data were acquired by markers mounted on some points on the human body and cameras with high motion capture sensitivity. As a result of the analysis of the images obtained from the cameras, it is possible to get the angular and linear kinematic variables of the limbs and joints. The obtained data are used as input data for humanoid robots or exoskeletons.

Almost all movements are considered to be periodic for the biological systems in nature and it is also valid for human gait [17,18]. When considered the movement of a leg, if the foot is on the ground, the movement is in the support phase. If the foot is in the air, the swing phase occurs. The support phase, which starts with the contact of the heel on the ground, ends at toe-off. The support phase takes about 60% of the gait cycle and the swing phase is about 40%. Since the gait cycle is considered to be symmetrical for the movement of the legs, the other leg performs the same phases of the movement with a phase difference. Thus, a complete walking cycle is completed [19].

In this paper, a 7-link dynamic model for bipedal walking is presented. The equations of motion of the system are obtained by Lagrange equations and a new approach that the COP of the foot is considered as an instantaneous center of rotation (IC). Using the kinematic data of experimental study [1], the joint torques are determined. Analytical solution results and torque results obtained in the experimental study are compared and evaluated.

2. METHODS

2.1 The Seven-Link Biped Model

The main purpose of the walking is to move the trunk forward. So, human walking takes place mainly in the sagittal plane. Based on this, this study focuses on the walking performed in the sagittal plane and the locomotions in other planes are neglected. The model is described in the sagittal plane.

The complex structure of the human skeletal system and the effects of the muscles during locomotion make a perfect simulation of the real human gait impossible. For this reason, some assumptions and idealizations are required. The following assumptions are made in the related models [1,20–23] in the literature; the mass of each limb is point mass, the point masses are located at the center of mass (COM) of each limb, the location of the COM of each limb is fixed during locomotion, all joints are assumed friction-free revolute joints, the moments of inertia of the limbs about the COMs, proximal ends and distal ends are constant during locomotion, the distance between the joints do not change and the limb lengths are constant, the friction between support foot and ground is enough to prevent slippage and also the locomotion is constrained in the sagittal plane.

According to these assumptions, the 7-link holonomic biped is modeled and illustrated in Fig. 1.

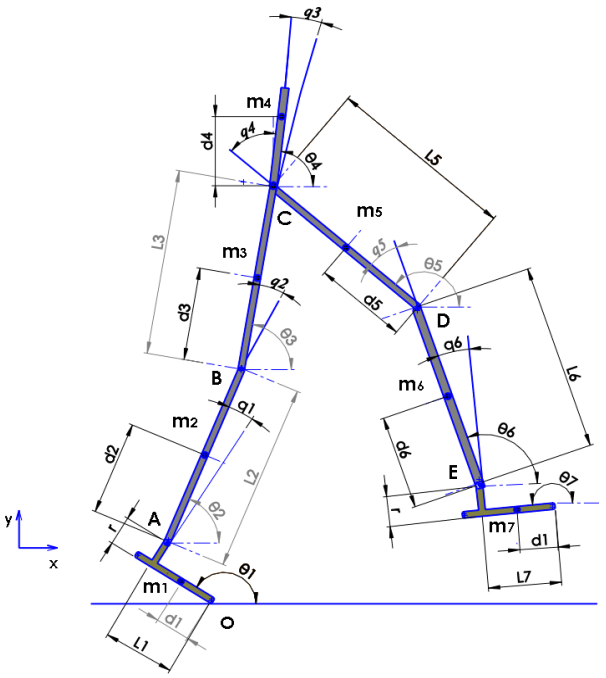

Figure.1. Structure of the bipedal model in the sagittal plane.

The vector of generalized coordinates of the model is $\theta = [\theta_1,\theta_2,\theta_3,\theta_4,\theta_5,\theta_6,\theta_7]^T$ and the vector of net joint angles is $q = [q_1,q_2,q_3,q_4,q_5,q_6,q_7]^T$. The origin of the inertial reference frame is point O. x-axis is the forward direction and y-axis is upward. The location of the center of mass for each link is shown as a point. It is focused on the single support phase (SSP) of gait. The model consists of 7 links which are 2 thighs, 2 shanks, 2 feet and the trunk. The link-1 of the model, the support foot, represents the right foot. The swing foot, the link-7, is the left foot. The head, arms and trunk (HAT) are not shown separately. The link-4 is studied as a single link which is the equivalent link of the HAT. The other links are shanks (link 2 and 6) and thighs (links 3 and 5). The shanks and

thighs are geometrically and inertially identical. In addition, each link is modeled as a rigid bar. The links are connected via 6 frictionless revolute joints which are 2 hips, 2 knees and 2 ankle joints. The friction between the ground and the support foot is considered too great to slip.

2.2 Kinetic Analysis of the Support Foot and Center of Pressure (COP)

The stance phase for human walking is the period of time that the foot is on the ground. The ground reaction forces act upon the support foot during its contact with the ground. The resultants of these forces (R_x and R_y) occur at the COP. Since the resultant forces act at the single point between the foot and the ground, this point can be assumed as a revolute joint between the foot and the ground. Accordingly, the COP is an instantaneous center of rotation (IC) of which location is varying from the heel to tip of the toe. The support foot rotates about these points. In Fig.1, the link-1 (support foot) rotates about point O which is the IC. So, this point is not the tip of the toe. It represents the COP at which the foot rotates without slipping. This joint can be called a hypothetical joint.

In the model, the support foot is evaluated as two parts. The first part is between the heel of the foot and the COP. The second part is between the COP and the tip of the toe. These parts are considered as rigid rods separately. The first is the part that rotates about the ground in the support phase. It is seen as the link-1 and included in the analysis. It is supposed that the second part of the foot is integrated with the ground in the support phase and behaves like a fixed link. This part is not included as a separate link and has no effect on the dynamics of the system.

L_1 refers to the distance between the heel and the COP. So it is a length that varies during the (SSP). According to that, the distance d_1, between the COP and the COM of the foot, also varies. On the other hand, since the foot in the swing phase has no contact with the ground, there is no external force. The situation mentioned for the support foot is invalid here. The length L_7 is fixed and corresponds to the distance between the heel and the toe.

Kinetic analysis of the support foot is done to specify the instantaneous location of the COP and L_1. The free-body diagram of the foot is given in Fig.2. A foot model similar to the foot of the 'foot-inverted pendulum model', which is used in the studies of Pai [24–26] and his group, is chosen. According to the model, the foot base is assumed completely in contact with the ground and remains stable during the support phase. The location of the ground reaction force vectors varies during the support phase.

The COM, the COP, the ankle torque T_1 and the reaction forces (R_x and R_y) are shown in the figure. The location of the COP is measured from the heel. L_f is the distance between the heel and the tip of the toe, c is the distance between the heel and the projection of the ankle on the base, d is the distance between the COM and the tip of the toe and r is the distance between the base of the foot and the ankle.

To define the COP and L_1, the torque about A;

$$\sum M_A = I_1.\alpha_1 \tag{1}$$

$$(COP - c).R_y + r.R_x + T_1 - (Lf - c - d).m.g = I_1.\alpha_1 \tag{2}$$

The position of the COP;

$$COP = \frac{I_1.\alpha_1 + (Lf - c - d).m.g - r.R_x - T_1}{R_y} + c \tag{3}$$

According to the Fig.2, L_1 as follows,

$$L_1 = COP - c \tag{4}$$

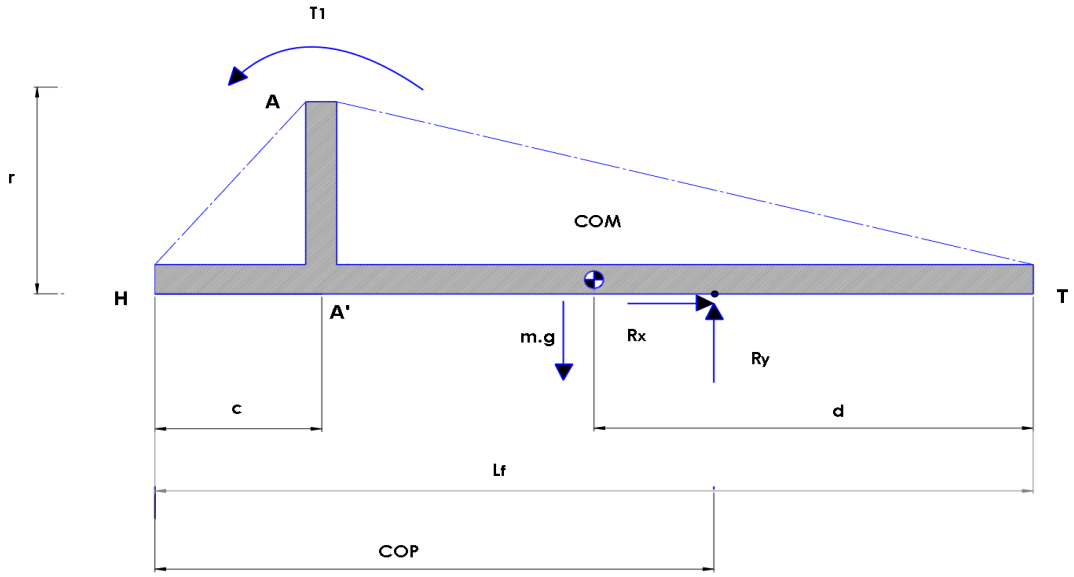

Figure.2. Schematic representation and free-body diagram of the support foot

2.3 Kinematic Analysis

For describing the model mathematically, kinematic analysis is required first. As a result of the analysis, the position and velocity of the links and the equations of motion of the system can be obtained.

The parameters of the model are as follows;

$\boldsymbol{\theta_i}$: Angle of link i with respect to the horizontal

$\boldsymbol{m_i}$: Mass of link i

$\boldsymbol{L_i}$: Length of link i

$\boldsymbol{d_i}$: Distance between COM of link i and the distal end

$\boldsymbol{I_i}$: Moment of inertia of link i with respect to the COM

x,y: Inertial reference frame

In the kinematic analysis, the positions the COMs are defined. The IC of the right foot between the ground, point O, is the origin of the coordinate system. The positions of the COMs of the links are given below;

$$x_{m1} = d_1.\cos\theta_1$$
$$y_{m1} = d_1.\sin\theta_1$$
$$x_{m2} = L_1.\cos\theta_1 + r.cos\left(\theta_1 - \left(\frac{\pi}{2}\right)\right) + d_2.\cos\theta_2$$
$$y_{m2} = L_1.\sin\theta_1 + r.sin\left(\theta_1 - \left(\frac{\pi}{2}\right)\right) + d_2.\sin\theta_2$$
$$x_{m3} = L_1.\cos\theta_1 + r.cos\left(\theta_1 - \left(\frac{\pi}{2}\right)\right) + L_2.\cos\theta_2 + d_3.\cos\theta_3$$
$$y_{m3} = L_1.\sin\theta_1 + r.sin\left(\theta_1 - \left(\frac{\pi}{2}\right)\right) + L_2.\sin\theta_2 + d_3.\sin\theta_3$$
$$x_{m4} = L_1.\cos\theta_1 + r.cos\left(\theta_1 - \left(\frac{\pi}{2}\right)\right) + L_2.\cos\theta_2 + L_3.\cos\theta_3 + d_4.\cos\theta_4$$
$$y_{m4} = L_1.\sin\theta_1 + r.sin\left(\theta_1 - \left(\frac{\pi}{2}\right)\right) + L_2.\sin\theta_2 + L_3.\sin\theta_3 + d_4.\sin\theta_4$$
$$x_{m5} = L_1.\cos\theta_1 + r.cos\left(\theta_1 - \left(\frac{\pi}{2}\right)\right) + L_2.\cos\theta_2 + L_3.\cos\theta_3 + (L_5 - d_5).\cos(\theta_5 + \pi)$$
$$y_{m5} = L_1.\sin\theta_1 + r.cos\left(\theta_1 - \left(\frac{\pi}{2}\right)\right) + L_2.\sin\theta_2 + L_3.\sin\theta_3 + (L_5 - d_5).\sin(\theta_5 + \pi)$$
$$x_{m6} = L_1.\cos\theta_1 + r.cos\left(\theta_1 - \left(\frac{\pi}{2}\right)\right) + L_2.\cos\theta_2 + L_3.\cos\theta_3 + L_5.\cos(\theta_5 + \pi) + (L_6 - d_6).\cos(\theta_6 + \pi)$$
$$y_{m6} = L_1.\sin\theta_1 + r.\sin\left(\theta_1 - \left(\frac{\pi}{2}\right)\right) + L_2.\sin\theta_2 + L_3.\sin\theta_3 + L_5.\sin(\theta_5 + \pi) + (L_6 - d_6).\sin(\theta_6 + \pi)$$
$$x_{m7} = L_1.\cos\theta_1 + r.cos\left(\theta_1 - \left(\frac{\pi}{2}\right)\right) + L_2.\cos\theta_2 + L_3.\cos\theta_3 + L_5.\cos(\theta_5 + \pi) + L_6.\cos(\theta_6 + \pi) + r.\cos\left(\theta_7 + \left(\frac{\pi}{2}\right)\right) + (L_7 - d_7).\cos(\theta_7 + \pi)$$
$$y_{m7} = L_1.\sin\theta_1 + r.sin\left(\theta_1 - \left(\frac{\pi}{2}\right)\right) + L_2.\sin\theta_2 + L_3.\sin\theta_3 + L_5.\sin(\theta_5 + \pi) + L_6.\sin(\theta_6 + \pi) + r.\sin\left(\theta_7 + \left(\frac{\pi}{2}\right)\right) + (L_7 - d_7).\sin(\theta_7 + \pi)$$

(5)

2.4 Equations of Motion

In many studies in the literature on mathematical modeling of the gait [20,27–29], Lagrange equations are used and important results are obtained. In this study, the equations of motion of the system are specified using the Lagrange equations in generalized coordinates. First of all, generalized coordinates are defined. Each of the links rotates about the z-axis which passing through the inertial frame perpendicular to the sagittal plane. The generalized coordinates of the system;

$$\theta = (\theta_1, \theta_2, \theta_3, \theta_4, \theta_5, \theta_6, \theta_7) \quad (6)$$

The generalized torques with respect to the generalized coordinates;

$$T = (T_1, T_2, T_3, T_4, T_5, T_6, T_7) \quad (7)$$

Each link in the system has gravitational potential energy. The potential energy of the system in terms of generalized coordinates;

$$U = U(\theta_1, \theta_2, \theta_3, \theta_4, \theta_5, \theta_6, \theta_7) \quad (8)$$

$$U = \sum_{i=1}^{7} (m_i.g.y_i) \quad (9)$$

Since the kinetic energies of the links depend on both generalized coordinates and velocities, the total kinetic energy of the system;

$$K = K(\theta_1, \theta_2, \theta_3, \theta_4, \theta_5, \theta_6, \theta_7, \dot{\theta}_1, \dot{\theta}_2, \dot{\theta}_3, \dot{\theta}_4, \dot{\theta}_5, \dot{\theta}_6, \dot{\theta}_7) \quad (10)$$

$$K = \sum_{i=1}^{7} \left(\frac{1}{2}.m_i.(\dot{x}_i^2 + \dot{y}_i^2) + \frac{1}{2}.I_i.\dot{\theta}_i^2\right) \quad (11)$$

According to the kinetic and potential energy, the Lagrangian;

$$L = K - U = L(\theta_1, \theta_2, \theta_3, \theta_4, \theta_5, \theta_6, \theta_7, \dot{\theta}_1, \dot{\theta}_2, \dot{\theta}_3, \dot{\theta}_4, \dot{\theta}_5, \dot{\theta}_6, \dot{\theta}_7) \quad (12)$$

Then, Lagrange equations of motion are obtained;

$$\frac{d}{dt}\left(\frac{\partial L}{\partial \dot{\theta}_i}\right) - \frac{\partial L}{\partial \theta_i} = T_i \quad , \qquad (\mathrm{i} = 1, \dots, 7) \quad (13)$$

The equations of motion are shown in matrix-vector form as follows;

$$A(\theta).\ddot{\theta} + C\left(\theta, \dot{\theta}\right) + G(\theta) = T_i \quad (14)$$

Where;

- $A(\theta) \in \Re^{7x7}$, Inertia Matrix
- $C\left(\theta, \dot{\theta}\right) \in \Re^{7}$, Coriolis/Centripetal Vector
- $G(\theta) \in \Re^{7}$, Gravitational Torque Vector
- T_i , Generalized Torque Vector

The generalized torque vector represents the resultant torques acting upon the links. Relative angles are needed to determine the joint torques. In Fig.1; the angles q_1, q_2, q_3, q_4, q_5 and q_6 show the joint angles. These angles are calculated as;

$$\begin{aligned} q_1 &= \theta_2 - \theta_1 + \frac{\pi}{2} \\ q_2 &= \theta_3 - \theta_2 \\ q_3 &= \theta_4 - \theta_3 \\ q_4 &= \theta_5 - \theta_4 \\ q_5 &= \theta_5 - \theta_6 \\ q_6 &= \theta_6 - \theta_7 + \frac{\pi}{2} \end{aligned} \quad (15)$$

The relationship between generalized torques and net joint torques can be expressed as;

$$T_i = \sum_{j=1}^{6} \tau_j . \frac{\partial q_j}{\partial \theta_i} \qquad i = 1, \dots, 7 \quad (16)$$

The matrix-vector form of the equation is;

$$T_i = E.\tau_j \quad (17)$$

Where, 7x6 Transformation matrix E is;

$$E = \begin{bmatrix} -1 & 0 & 0 & 0 & 0 & 0 \\ 1 & -1 & 0 & 0 & 0 & 0 \\ 0 & 1 & -1 & 0 & 0 & 0 \\ 0 & 0 & 1 & -1 & 0 & 0 \\ 0 & 0 & 0 & 1 & -1 & 0 \\ 0 & 0 & 0 & 0 & 1 & -1 \\ 0 & 0 & 0 & 0 & 0 & 1 \end{bmatrix} \quad (18)$$

2.5 Normal Gait Trials

Kinematic data of the links, inertia matrix elements, Coriolis / centripetal vector and gravity vector elements must first be determined in order to get joint torques,. Also, ground reaction forces are required to determine the position of the COP.

Kinetic, kinematic and anthropometric data, obtained in CGA conducted by Winter [1], are used in this study for that. Besides these experiments, no other experiment has not been done. In the CGA, the normal gait of a 56.7 kg healthy individual on the ground with force plates is examined. The gait cycle duration is 1 second. Eight anatomical markers are used to measure all kinematic data of the subject's limbs. Markers are mounted on the rib cage, right hip joint, right knee joint, right ankle joint, heel, right 5th metatarsal joint and the right toe. During the gait, these markers are monitored by sensitive cameras and the coordinates of the points are recorded. 70 frames are taken during the 1s cycle. 27 of them are in the SSP, 27 of them are in the swing phase and 16 of them are in the double support phase (DSP), for one of the foot. All kinematic data are acquired by processing on the computer. Also, measurements of the ground reaction forces are taken by

force plates. The joint forces and the joint torques are determined by the analysis of these forces and presented in the tables. Details of the experimental study can be found in [1].

The 1-second gait cycle is analyzed for the right lower extremities and the trunk. 0.386 seconds of the cycle is occurred in the SSP, 0.386 seconds in the swing phase and 0.228 seconds in the DSP. The left foot follows the same motion profile delayed half second.

The weights of the extremities of a healthy person, the positions of the COMs and the radius of gyrations are compiled by Winter [1] from his experimental studies and other several investigators' studies [30,31] on cadavers and given in table 1. Limb weights are expressed as the ratio of the total body weight. The positions of the COMs are given from the distal and proximal ends and as a ratio of the length of the limbs. The gyration radius as a ratio of the related segment length is shown in the table for the COM, the proximal end and the distal end.

Table 1. Anthropoetric Data of Lower Limbs

Segment	Segment Weight / Total Body Weight	Center of Mass/ Segment Length		Radius of Gyration/ Segment Length		
		Proximal	Distal	Center of Mass	Proximal	Distal
Foot (Lateral malleolus /head metatarsal II)	0.0145	0.5	0.5	0.475	0.69	0.69
Shank (Femoral condyles / medial malleolus)	0.0465	0.433	0.567	0.302	0.528	0.643
Thigh (Greater trochanter / femoral condyles)	0.1	0.433	0.567	0.323	0.54	0.653
Head, Arms and Trunk (HAT) (Grater trochanter/mid rib)	0.678	1.142	-	0.903	1.456	-

3. RESULTS

3.1 Position of the Center of Pressure (COP)

The equation giving the position of the COP has already been defined in equation 3. By using all required data measured in the normal gait experiments; the graph of the COP versus time is depicted in Fig. 3.

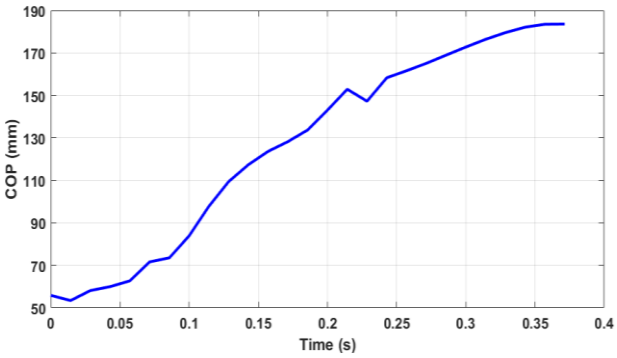

Figure. 3. Location of the center of pressure (COP) during the single support phase (SSP) in the horizontal axis

The position of the COP starts approximately 50 mm distance from the heel. The reason for this is that while the COP is in the range of 0-50 mm, the gait is in the DSP. Then, the SSP begins. According to Fig.3 in the SSP, the COP location generally progresses towards the toe over time. However, there is a slight drop between 0.2 and 0.25 s and then continues to progress. The reason is that the direction of the horizontal reaction force acting on the sole, Rx, changes from anterior to posterior direction. When the COP is around 190 mm, the other DSP starts again. Accordingly, the approximate location of the COP on the base of the individual is shown in Fig.4.

The position of the COP progresses from the heel to a little further of ankle projection in the first 11.4% range of the cycle time. This process takes place in the DSP. Between 11.4% and 50% of the gait cycle is the time spent in the SSP. In Fig.4, the COP is in the region between the red solid arrows. The COP is beyond the 5th

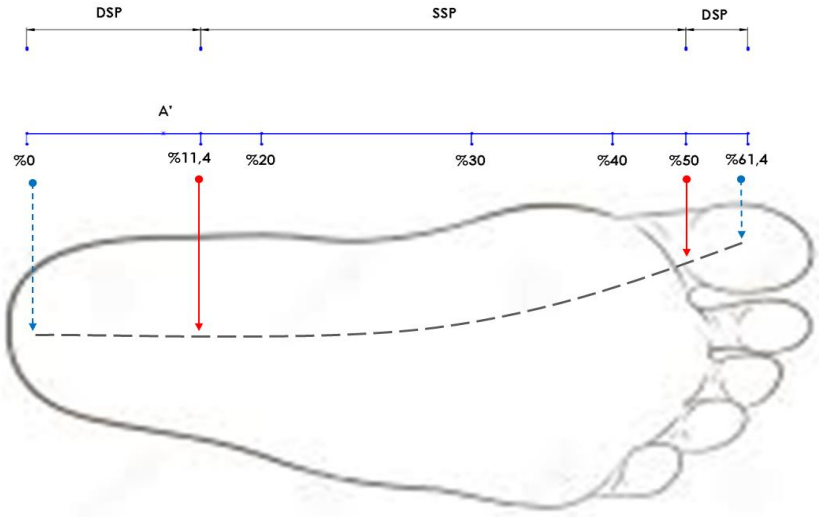

Figure.4. Progression of the location of the center of pressure (COP) on the base of the support foot.

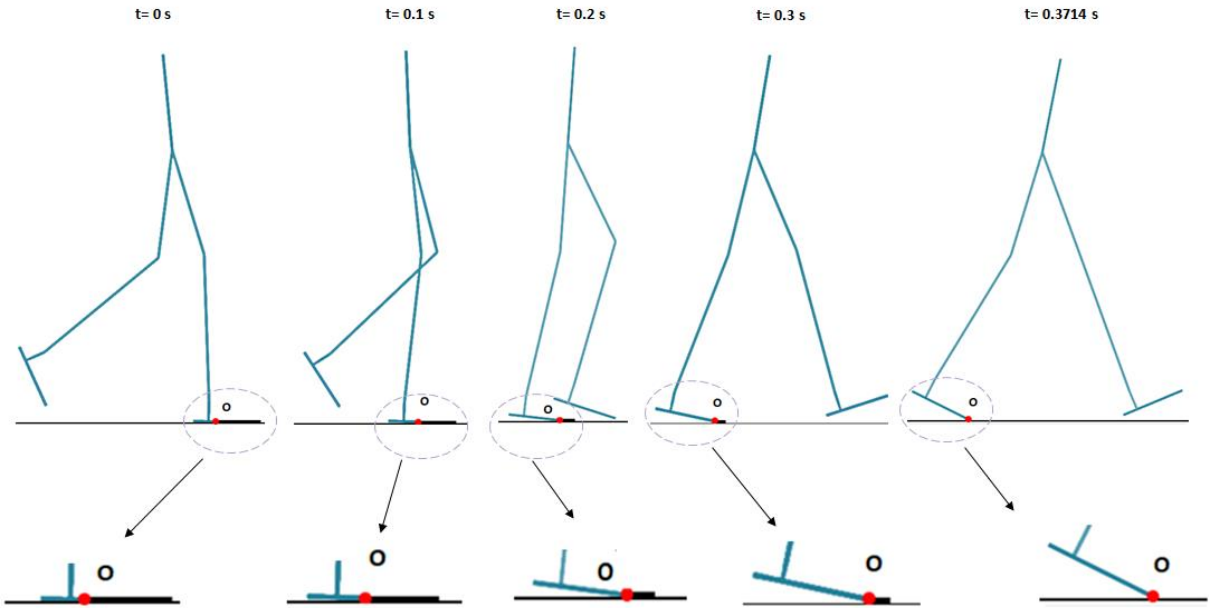

Figure.5. Schematic representation of the rotation of the support foot about COP during the SSP

Table 2. Physical parameters of the biped model.

Link No i	**Mass m_i (kg)**	**Length L_i (m)**	**Center of Mass d_i (m)**	**Moment of Inertia I_i ($kg.m^2$)**
1	0.82	varies with time (from 0.0101 to 0.1403)	varies with time (from 0.0051 to 0.0701)	varies with time (from $1.3x10^{-5}$ to $2.5x10^{-3}$)
2,6	2.63	0.425	0.241	0.0434
3,5	5.67	0.314	0.178	0.0583
4	38.44	0.25	0.286	1.9592
7	0.82	0.184	0.092	0.0062

metatarsal joint and under the toe at the end of the SSP. Between 50% and 61.4% of the cycle, the gait is in the second DSP. When the COP is on the toe, the foot cuts off the contact with the ground and begins to swing. According to Fig. 3 and 4, a representative simulation of the bipedal model and position of the support foot are illustrated in Fig.5. The support foot is presented in two parts. The first part is between the heel of the foot and the COP. The second part is between the COP and the tip of the toe. Point O indicates the COP of the support foot and the first part rotates about this point. This part is considered as the link-1 on the model in Fig.1. The second part of the foot is supposed to be a passive link and behaves like fixed during the SSP.

3.2 Calculation of the Joint Torques and Comparison

Equations of motion have been obtained by applying Lagrange equations and given by equations (14) - (18) above. Most of the physical parameters in these equations are determined according to the dimensions of the individual and the anthropometric data of CGA[1]. The length of link-1 (L_1), the position of the COM (d_1) and the moment of inertia (I_1) are calculated according to the varying position of the center of pressure (COP). All physical parameters are presented in table 2.

By using the kinematic data and the physical parameters, equations of motions are solved with Matlab and analytical results are obtained. Comparative graphs of analytically determined joint torques and experimental joint torques of CGA[1] are given in Fig.6. The values are normalized relative to the total body mass. The blue (solid line) curves represent the analytically obtained joint torques. The red (dashed line) is experimentally derived joint torques of CGA[1].

According to the graphs in Fig.6, although some errors are observed, the analytical results have good agreement with the experimental measurements. The results calculated for the right and left ankle joints are much closer to the actual values, which are compared to the results of the other joints on the same side of the lower extremities. Considering the COP of the support foot as an IC gives better results, especially for the right (support) ankle. In the last part of the right ankle graph,

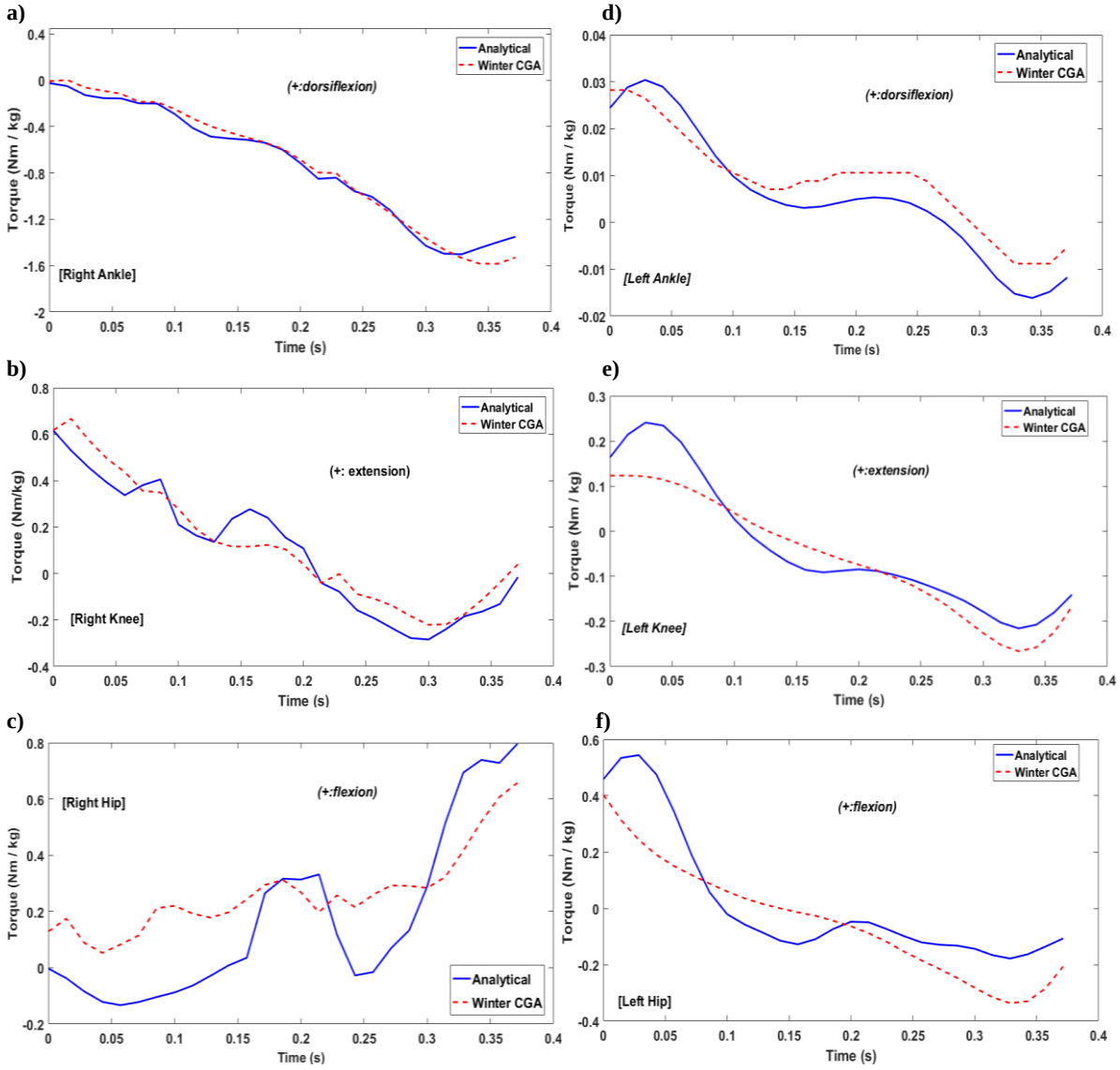

Figure.6. Torque curves of the right/stance ankle (a), right/stance knee (b), right/stance hip (c), left/swing ankle (d), left/swing knee (e), left/swing hip (f).

it can be seen that the error started to increase. The largest error value reaches 0.186 Nm / kg. This is because the COP passes beyond the first metatarsal joint (metatarsophalangeal), which is the joint between the metatarsal bone of the foot and the proximal bone of the toe. In that case, L_1 and d_1 parameters of the dynamic model are miscalculated. Due to this, errors are observed. The error in the left ankle results is the smallest compared to all other joints.

If the joints are classified as right and left joints in the evaluations, it can be seen that the error in the right knee joint is larger than the right ankle error, and the error in the right hip joint is larger than the right knee joint error. The same is true for left side joints. According to equations 15, 16 and 17; the joint torques can be defined with respect to generalized torques. Ankle torque values are equal to the generalized torque values of feet.

However, the situation is different for knee and hip joint torques. Knee joint torques are calculated from generalized torque values of the foot and shank (links 1,2 / links 7,6). The hip joints torques depend on the generalized torque values of the foot, shank and thigh (links 1,2,3 / links 7,6,5). As a result, the sum of minor errors in generalized torque values turns into large errors in the upper joint torques. Therefore, the errors increase from the lower joints to the upper.

The following table is created to better examine all results. The evaluation of analytical results according to experimental results is summarized. The root mean square error (RMSE) and maximum error values are presented. The RMSE and the maximum error are computed to assess the accuracy of the new analytical approach. These are used as the error indicators between the analytical and experimental results.

Table 3. Evaluation of the analytical results according to the experimental data.

	Right (Stance)		Left (Swing)	
Joints	**RMSE**	**Max. Error**	**RMSE**	**Max. Error**
Hip	0.1973	0.277	0.1339	0.301
Knee	0.0874	0.176	0.0534	0.119
Ankle	0.0701	0.186	0.0051	0.006

4. CONCLUSION

An alternative dynamic model is developed for bipedal gait, in this study. The model consists of feet, lower legs (shanks), upper legs (thighs) and trunk. The links are considered as rigid bars and connected via rotating joints. Kinematic analysis of the model is done and the links are sized according to real anthropometric data. The equations of motion are obtained by Lagrange equations and given in the matrix-vector form.

The resultants of ground reaction forces occur on the foot in the COP. It is supposed that this point is a hypothetical revolute joint between the foot and the ground and the foot rotates about this point in the SSP. The location of the COP is continuously moving from the heel to the tip of the toe, horizontally. Hence, this point can be defined as an IC and shown in Fig.5. While solving the equations of motion, this assumption is taken into consideration and 27 different COPs are determined during the SSP. The equations are solved for 27 different L_1 and d_1 lengths. L_1 refers to the distance between the heel and the COP and considered as the length of the link-1. It is assumed that the part between the COP and the toe of the foot is horizontally on the ground and does not rotate.

The results of the clinical gait analysis conducted by Winter are used to verify the mathematical model. The torque values of the ankle, knee and hip joints are determined. The analytical results are compared with the experimental joint torque values.

Although there are differences between analytical and experimental results, close resemblances in the comparisons are found. These differences arise from the idealizations and some negligence made during the creation of the model and analysis. It is seen that analytical solutions for ankles give better results compared to solutions for other joints. Especially, the fact that the torque values of the support ankle are so good reveals how successful the approach that the COP is an IC is. The increment of the error in the last part of the graph shows that this assumption works in the part of the foot up to the 1st metatarsal (metatarsophalangeal) joint.

The RMSE of the right knee joint torque is higher than the RMSE of the right ankle and the RMSE of the right hip joint torque is also greater than the RMSE of the right knee joint. These determinations are also valid for left joints. The reason is that the errors in the lower joints increase the errors in the upper joints consecutively.

DECLARATION OF ETHICAL STANDARDS

The author(s) of this article declare that the materials and methods used in this study do not require ethical committee permission and/or legal-special permission.

AUTHORS' CONTRIBUTIONS

Fatih CELLEK: Analysed the results and wrote the manuscript

Bariş KALAYCIOĞLU: Analysed the results.

CONFLICT OF INTEREST

There is no conflict of interest.

REFERENCES

[1] Winter, D. A., "Biomechanics and Motor Control of Human Movement", 4. Ed., ***John Wiley & Sons, Inc.***, Hoboken, NJ, USA, (2009).

[2] Ito, D., Murakami, T., and Ohnishi, K., "An Approach to Generation of Smooth Walking Pattern for Biped Robot", ***International Workshop on Advanced Motion Control, AMC***, Maribor, Slovenia, 98–103 (2002).

[3] Chen, B., Ma, H., Qin, L. Y., Gao, F., Chan, K. M., Law, S. W., Qin, L., and Liao, W. H., "Recent developments and challenges of lower extremity exoskeletons", ***Journal Of Orthopaedic Translation***, 5: 26–37 (2016).

[4] Viteckova, S., Kutilek, P., and Jirina, M., "Wearable lower limb robotics: A review", ***Biocybernetics And Biomedical Engineering***, 33 (2): 96–105 (2013).

[5] Bakırcıoğlu, V. and Kalyoncu, M., "A literature review on walking strategies of legged robots", ***Journal Of Polytechnic***, 23 (4): 961–986 (2019).

[6] Oh, S. N., Kim, K. Il, and Lim, S., "Motion Control of Biped Robots Using a Single-Chip Drive", ***IEEE International Conference on Robotics and Automation***, Taipei, Taiwan, 2461–2465 (2003).

[7] Chevallereau, C., Bessonnet, G., Abba, G., and Aoustin, Y., "Bipedal Robots : Modeling, Design and Walking Synthesis", ***ISTE***, London, UK, (2009).

[8] Dollar, A. M. and Herr, H., "Lower Extremity Exoskeletons and Active Orthoses: Challenges and State-of-the-Art", ***IEEE Transactions On Robotics***, 24 (1): 144–158 (2008).

[9] Ji, Z. and Manna, Y., "Synthesis of a pattern generation mechanism for gait rehabilitation", ***Journal Of Medical Devices, Transactions Of The ASME***, 2 (3): (2008).

[10] Dillmann, R., Albiez, J., Gaßmann, B., Kerscher, T., and Zöllner, M., "Biologically inspired walking machines: Design, control and perception", ***Philosophical Transactions Of The Royal Society A: Mathematical, Physical And Engineering Sciences***, 365 (1850): 133–151 (2007).

[11] Pfeiffer, F. and Inoue, H., "Walking: Technology and biology", ***Philosophical Transactions Of The Royal Society A: Mathematical, Physical And Engineering Sciences***, 365 (1850): 3–9 (2007).

[12] Kirtley, C., "Clinical Gait Analysis: Theory and Practice.", 1. Ed., ***Elsevier Churchill Livingstone***, London, 316 (2006).

[13] Popovic, M. B., Goswami, A., and Herr, H., "Ground Reference Points in Legged Locomotion: Definitions, Biological Trajectories and Control Implications", ***The International Journal Of Robotics Research***, 24 (12): 1013–1032 (2005).

[14] Jung, W. C. and Lee, J. K., "Treadmill-to-overground mapping of marker trajectory for treadmill-based continuous gait analysis", ***Sensors***, 21 (3): 1–13 (2021).

[15] Nagymáté, G. and Kiss, R. M., "Affordable gait analysis using augmented reality markers", ***PLoS ONE***, 14 (2): (2019).

[16] Haque, M. R., Imtiaz, M. H., Kwak, S. T., Sazonov, E., Chang, Y. H., and Shen, X., "A lightweight exoskeleton-based portable gait data collection system†", ***Sensors***, 21 (3): 1–17 (2021).

[17] Cruse, H., Kindermann, T., Schumm, M., Dean, J., and Schmitz, J., "Walknet - A biologically inspired network to control six-legged walking", ***Neural Networks***, 11 (7–8): 1435–1447 (1998).

[18] Huang, Q., Yokoi, K., Kajita, S., Kaneko, K., Aral, H., Koyachi, N., and Tanie, K., "Planning walking patterns for a biped robot", ***IEEE Transactions On Robotics And Automation***, 17 (3): 280–289 (2001).

[19] Zoss, A. and Kazerooni, H., "Design of an electrically actuated lower extremity exoskeleton", ***Advanced Robotics***, 20 (9): 967–988 (2006).

[20] Tzafestas, S., Raibert, M., and Tzafestas, C., "Robust sliding-mode control applied to a 5-link biped robot", ***Journal Of Intelligent And Robotic Systems: Theory And Applications***, 15 (1): 67–133 (1996).

[21] Pournazhdi, A. B., Mirzaei, M., and Ghiasi, A. R., "Dynamic Modeling and Sliding Mode Control for Fast Walking of Seven-Link Biped Robot", ***2nd International Conference on Control, Instrumentation and Automation (ICCIA)***, Shiraz, Iran, 1012–1017 (2011).

[22] Onn, N., Hussein, M., Howe, C., Tang, H., Zain, M. Z., Mohamad, M., and Ying, L. W., "Motion Control of Seven-Link Human Bipedal Model", ***14th International Conference on Robotics, Control and Manufacturing Technology(ROCOM'14)***, 15–22 (2014).

[23] Paparisabet, M. A., Dehghani, R., and Ahmadi, A. R., "Knee and torso kinematics in generation of optimum gait pattern based on human-like motion for a seven-link biped robot", ***Multibody System Dynamics***, 47 (2): 117–136 (2019).

[24] Pai, Y. C. and Iqbal, K., "Simulated movement termination for balance recovery: Can movement strategies be sought to maintain stability in the presence of slipping or forced sliding?", ***Journal Of Biomechanics***, 32 (8): 779–786 (1999).

[25] Pai, Y. C., Maki, B. E., Iqbal, K., McIlroy, W. E., and Perry, S. D., "Thresholds for step initiation induced by support-surface translation: A dynamic center-of-mass model provides much better prediction than a static model", ***Journal Of Biomechanics***, 33 (3): 387–392 (2000).

[26] Pai, Y. C. and Patton, J., "Center of mass velocity-position predictions for balance control", ***Journal Of Biomechanics***, 30 (4): 347–354 (1997).

[27] Mu, X. and Wu, Q., "Development of a complete dynamic model of a planar five-link biped and sliding mode control of its locomotion during the double support phase", ***International Journal Of Control***, 77 (8): 789–799 (2004).

[28] Ha, S., Han, Y., and Hahn, H., "Adaptive gait pattern generation of biped robot based on human's gait pattern analysis", ***International Journal Of Mechanical Systems Science And Engineering***, 1 (2): 80–85 (2007).

[29] Hemami, H. and Farnsworth, R. L., "Postural and Gait Stability of a Planar Five Link Biped by Simulation", ***IEEE Transactions On Automatic Control***, 22 (3): 452–458 (1977).

[30] Miller, D. I. ; Nelson, R. C., "Biomechanics of Sport", ***Lea And Febiger***, Philadelphia, (1973).

[31] Plagenhoef, S., "The Patterns of Human Motion", ***Prentice-Hall***, Englewood Clifis, N.J, (1971)